Crystal Structure of $[Ru(terpy)_2]^0$: A New Crystalline Material from the Reductive Electrocrystallization of $[Ru(terpy)_2]^{2+}$

Soomi Pyo,[†] Eduardo Pérez-Cordero,[†] Simon G. Bott,[‡] and Luis Echegoyen*,[†]

Departments of Chemistry, University of Miami, Coral Gables, Florida 33124, and University of Houston, Houston, Texas 77204

Received December 7, 1998

Reductive electrocrystallization of $[Ru(terpy)_2](PF_6)_2$ (where terpy = 2,2′:6′,2″-terpyridine) from an acetonitrile solution containing 100 mM $TBAPF_6$ results in the formation of black crystals. Crystal data: $[Ru(terpy)_2]\cdot(PF_6)_2\cdot[(CH_3)_2CO]$, monoclinic, space group $P2_1/c$ with a = 20.801(2) Å, b = 8.943(1) Å, c = 19.453(2) Å, β = 92.524(9)°, and Z = 4; $[Ru(terpy)_2]$ (**1**), orthorhombic, $Fdd2$ with a = 39.757(4) Å, b = 56.464(6) Å, c = 8.507(1) Å, and Z = 32. X-ray analysis reveals that the crystals consist exclusively of $[Ru(terpy)_2]^0$ (**1**), with no solvent or counteranion present in the lattice. $[Ru(terpy)_2]^0$ units are structurally very similar to the parent $[Ru(terpy)_2]^{2+}$, with nearly perfect octahedral symmetry around the metal center and with two terpy ligands that are basically planar. Analysis of the crystal packing shows that $[Ru(terpy)_2]^{2+}$ crystals have close intermolecular distances, while $[Ru(terpy)_2]^0$ crystals show only intermolecular interactions along the c axis with contacts that are less than 3.5 Å. Analysis of molecular volumes and empty spaces reveals the presence of cavities, which could contain substantial electron density.

Introduction

In the past few years, we have been studying the preparation and properties of crystalline materials derived from reduced transition-metal complexes by electrocrystallization.[1−4] These materials can be visualized as "pseudoatom" species, which contain a cationic metal core surrounded by electrons that balance the charge, and are delocalized over a pseudospherical ligand system.[5] The first reported structure of this kind was called sodio cryptatium $[Na \subset (bpy_3)]^0$, a crystalline material derived from the reductive electrocrystallization of the sodium cryptate $[Na \subset (bpy_3)]^+Br^-$ (where (bpy_3) = tris-2,2′-bipyridyl cryptand), see structure in Chart 1. The electron in $[Na \subset (bpy_3)]^0$ is localized on one of the bipyridine units, as deduced from X-ray structure results.[6] Chart 1 shows the chemical structure of this cryptatium along with a sodium atom (left) and an electride (right). The cryptatium represents an intermediate state between the atom, where the 3s electron is held close to the nucleus, and the electride, where the electron is totally expelled from the ligand−cation complex.[7]

Chart 1

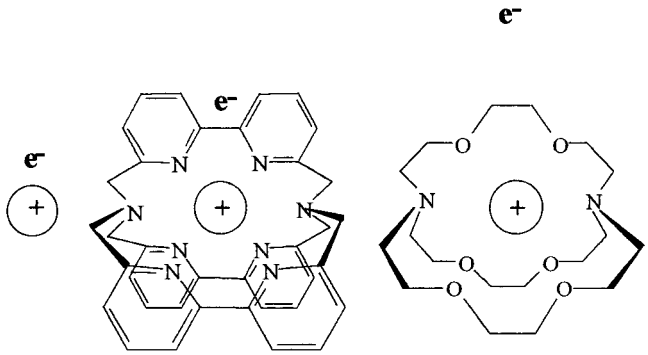

Recently, our group obtained single crystals of $[M(bpy)_3]^0$ (where M = Fe, Ru, and Os and bpy = bipyridine) by reductive electrocrystallization (Chart 2).[1,4] Compositional and structural characterization of these materials has been done by combustion microanalyses, ^{1}H NMR, ESR, and X-ray diffraction. The single-crystalline material $[Ru(bpy)_3]^0$ showed a good conductivity ($\sigma \approx 1.5 \times 10^{-1}\ \Omega^{-1}\ cm^{-1}$ at 297 K) along the c axis.[2] Also, reductive electrocrystallization of $[Ru(binap\text{-}2)_3](PF_6)_2$ (where binap-2 = 3,3′-dimethylene-2,2′-bi[1,8]naphthyridine) resulted in the formation of the one electron reduction product $[Ru(binap\text{-}2)_3](PF_6)$, which has one fewer PF_6^- per molecule unit compared with the parent compound (Chart 2).[3] The result of conductivity measurements indicated that the reduced material $[M(binap\text{-}2)_3](PF_6)$ is a semiconductor with a 0.53 eV band gap. All of these species are conceptually related to cryptatium and to endohedral fullerenes ($M^{n+}@C_{60}{}^{n-}$).[8] The latter have also been called "expanded atoms", where the ligand (C_{60}) is rigid and perfectly spherical. Endohedral fullerenes such as $La@C_{82}$ have been described as consisting of a central metal ion surrounded by a triply negative C_{82}, forming $La^{3+}@C_{82}{}^{3-}$.[8]

Although the terdentate ligand 2,2′:6′,2″-terpyridine was first isolated in 1937 by Morgan and Burstall,[9] not many crystal-

[†] University of Miami.
[‡] University of Houston.

(1) Pérez-Cordero, E.; Buigas, R.; Brady, N.; Echegoyen, L. *Helv. Chim. Acta* **1994**, *77*, 1222.
(2) Wagner, M. J.; Dye, J. L.; Pérez-Cordero, E.; Buigas, R.; Echegoyen, L. *J. Am. Chem. Soc.* **1995**, *117*, 1318.
(3) Pérez-Cordero, E.; Brady, N.; Echegoyen, L.; Thummel, R.; Hung, C.; Bott, S. G. *Chem.—Eur. J.* **1996**, *2*, 781.
(4) Pérez-Cordero, E.; Campana, C.; Echegoyen, L. *Angew. Chem., Int. Ed. Engl.* **1997**, *36*, 137.
(5) (a) Echegoyen, L.; Xie, Q.; Pérez-Cordero, E. *Pure Appl. Chem.* **1993**, *65*, 441. (b) Echegoyen, L.; Pérez-Cordero, E.; de Vains, J.-B. R.; Roth, C.; Lehn, J.-M. *Inorg. Chem.* **1993**, *32*, 572.
(6) Echegoyen, L.; DeCian, A.; Fischer, J.; Lehn, J.-M. *Angew. Chem., Int. Ed. Engl.* **1991**, *30*, 838.
(7) (a) Tehan, F. J.; Barnett, B. L.; Dye, J. L. *J. Am. Chem. Soc.* **1974**, *96*, 7203. (b) Dye, J. L. *Science* **1990**, *24*, 663. (c) Dye, J. L. *Chemtracts: Inorg. Chem.* **1993**, *5*, 243. (d) Dye, J. L. *Inorg. Chem.* **1997**, *36*, 3816.

10.1021/ic981395e CCC: $18.00
Published on Web 06/10/1999

Chart 2

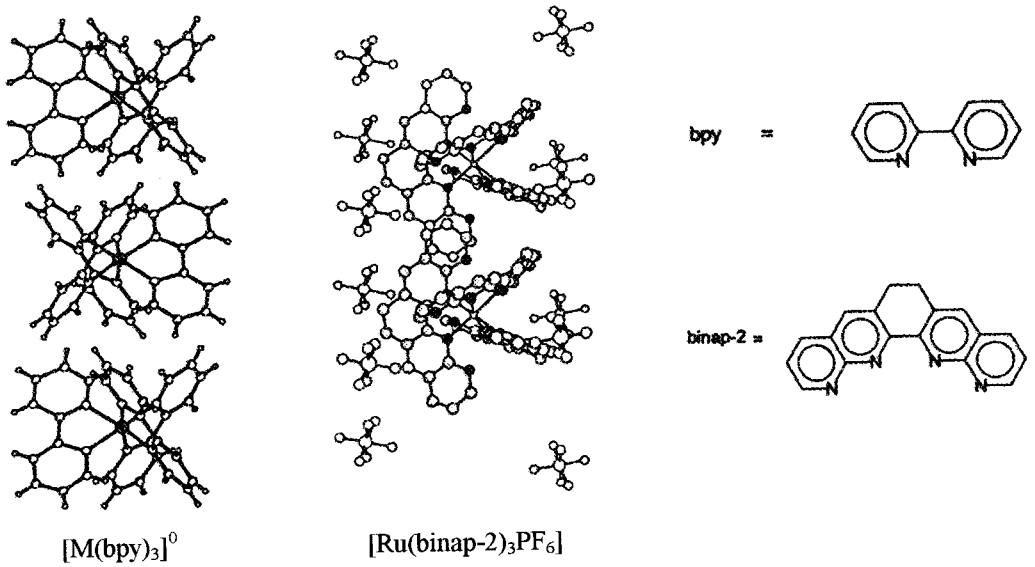

lographic studies of its complexes have been published.[10] The crystal structures of the complexes $[M(terpy)_2]^{2+}$ with M = Co, Cu, Fe, and Mg have been reported,[11−14] but, to our knowledge, crystallographic studies of $[Ru(terpy)_2]^{2+}$ have not appeared in the literature. In this work, we report the preparation and chemical characterization of new single crystals of electroneutral $[Ru(terpy)_2]^0$ (**1**) from $[Ru(terpy)_2](PF_6)_2$ by reductive electrocrystallization (where terpy = 2,2′:6′,2″-terpyridine). We also report the X-ray crystal structure of $[Ru(terpy)_2](PF_6)_2[(CH_3)_2CO]$ for the first time. The structure is compared with that of $[Ru(bpy)_3]^0$.

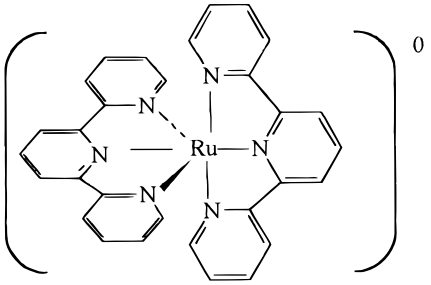

1

Experimental Section

General Procedure. All chemicals used were reagent grade unless otherwise specified. The complex $[Ru(terpy)_2](PF_6)_2$ was synthesized as previously reported.[15]

Table 1. Crystallographic Data for $[Ru(terpy)_2]^{2+}$ and $[Ru(terpy)_2]^0$ (**1**)

compd	**1**·$(PF_6)_2[(CH_3)_2CO]$	**1**
formula	$C_{33}H_{28}F_{12}N_6OP_2Ru$	$C_{30}H_{22}N_6Ru$
fw (g/mol)	915.63	567.62
space group	$P2_1/c$	$Fdd2$
Z	4	32
a (Å)	20.801(2)	39.757(4)
b (Å)	8.943(1)	56.464(6)
c (Å)	19.453(2)	8.507(1)
α (deg)	90.0	90.0
β (deg)	92.524(9)	90.0
γ (deg)	90.0	90.0
V (Å^3)	3615.2(7)	19097.0(4)
ρ_c (g/cm^3)	1.682	1.579
μ (cm^{-1})	6.05	6.75
F(000)	1832	9216
T (K)	298	298
radiation (λ, Å)	Mo Kα (0.7073)	Mo Kα (0.719 73)
final R indices[a] [$I > 6\sigma(I)$]	$R = 0.0586$	$R = 0.0372$
	$R_w = 0.0623$	$R_w = 0.0412$

[a] $R = \sum|F_o - F_c|/\sum|F_o|$ and $R_w = [\sum w(F_o^2 - F_c^2)^2/\sum wF_o^4]^{1/2}$, where $w = [0.04F^2 + (\sigma F)^2]^{-1}$.

Electrocrystallization. As described previously for $[Ru(bpy)_3]^{2+}$,[1] crystals of **1** were grown on a Pt electrode by reduction from a 2 mM $[Ru(terpy)_2](PF_6)_2$ complex in an acetonitrile (from Fisher) solution containing 100 mM tetrabutylammonium hexafluorophosphate (from Fluka). The process was carried under high vacuum (10^{-6} Torr) after the solvent was dried over P_4O_{10}, degassed by three freeze−pump−thaw cycles, and vapor transferred into the modified H-cell. The electrocrystallization was performed using a two-electrode configuration at a constant current density (11 μA/cm^2).[1]

Crystal Structure Determination. For the structural determination of **1**·$(PF_6)_2[(CH_3)_2CO]$ and **1**, a Siemens Enraf-Nonius CAD-4F diffractometer was used to collect the data using Mo Kα radiation. Because **1** is very air sensitive, a single crystal was coated with Paratone-N oil under an argon atmosphere and immediately placed in a cold nitrogen stream at 153 K on the X-ray diffractometer. Data collection and crystal parameters are summarized in Table 1. The structures were solved by a direct method using the program SHELXTL-XP.

(8) (a) Johnson, R. D.; de Vries, M. S.; Salem, J.; Bethune, D. S.; Yannoni, C. S. *Nature* **1992**, *355*, 239. (b) Weaver, J. H.; Chai, Y.; Kroll, G. H.; Jin, C.; Ohno, T. R.; Haufler, R. E.; Guo, T.; Alford, J. M.; Conceicao, J.; Chibante, L. P. F.; Jain, A.; Palmer, G.; Smally, R. E. *Chem. Phys. Lett.* **1992**, *190*, 460. (c) Bethune, D. S.; Johnson, R. D.; Salem, J. R.; de Vries, M. S.; Yannoni, C. S. *Nature* **1993**, *366*, 123. (d) Yamamoto, K.; Funasaka, H.; Takahashi, T.; Akasaka, T. *J. Phys. Chem.* **1994**, *98*, 2008.
(9) Morgan, G.; Burstall, F. H. *J. Chem. Soc.* **1937**, 1649.
(10) (a) Constable, E. C. *Adv. Inorg. Chem. Radiochem.* **1986**, *30*, 69. (b) Constable, E. C. *Tetrahedron* **1992**, *48*, 10013.
(11) Maslen, E. N.; Raston, C. L.; White, A. H. *J. Chem. Soc., Dalton Trans.* **1974**, 1803.
(12) Allmann, R.; Henke, W.; Reinen, D. *Inorg. Chem.* **1978**, *17*, 378.
(13) Baker, A. T.; Goodwin, H. A. *Aust. J. Chem.* **1985**, *38*, 207.
(14) Constable, E. C.; Healy, J.; Drew, M. G. B. *Polyhedron* **1991**, *10*, 1883.
(15) (a) Ciantelli, G.; Legittimo, P.; Pantani, F. *Anal. Chim. Acta* **1971**, *53*, 303. (b) Lytle, F. E.; Petrosky, L. M.; Carlson, L. R. *Anal. Chim. Acta* **1971**, *57*, 239. (c) Stone, M. L.; Crosby, G. A. *Chem. Phys. Lett.* **1981**, *79*, 169.

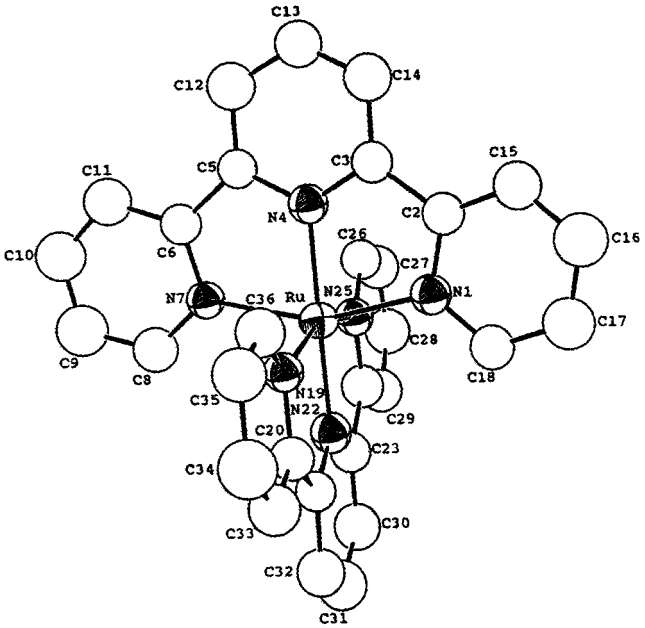

Figure 1. ORTEP view of a $[Ru(terpy)_2]^{2+}$ unit of unreduced compound **1**. The hydrogens have been omitted for clarity. Thermal ellipsoids are drawn at 50% probability.

VOID Fortran Program.[16] The VOID Fortran program calculates the cavity and channel structures; it is a useful connection tool between the structure modeling software (SHELXTL-XP) and the 3D isosurface software (EXPLORER). The grid-point program used is typically 40 × 40 × 40 points from 0 to 255 depending on the distance of the point from the nearest van der Waals surface. The program "xeo" was used to display the empty cavities and channels, and the program "zeo" displays the atomic or molecular surfaces. The output data of coarse isosurfaces are touched up with the "smooth" program to provide smoothed pictures of the molecular surfaces. The 3D viewing program EXPLORER was used with a Silicon Graphics computer to display 3D isosurface plots in order to determine the diameters of spheres and the dimensions of the various channels and cavities.

Results and Discussion

Crystal Structure of $1\cdot(PF_6)_2[(CH_3)_2CO]$. Compound $1\cdot(PF_6)_2[(CH_3)_2CO]$ (unreduced **1**) was crystallized from acetone by ether vapor transfer. The crystal system is monoclinic with space group $P2_1/c$. A red rod-shaped crystal (0.12 × 0.13 × 0.32 mm) was chosen. One unique molecular structure is found in the unit cell, shown in Figure 1. The angle of N4−Ru−N22 is 177.5°. Thus the two terpyridines are tilted 2.5° away from perfect orthogonality. Selected bond lengths and angles are summarized in Table 2. The two terpyridine ligands are substantially similar and perfectly planar for unreduced compound **1**. The mean deviations from the planes of each terpyridine ligand are 0.0218 and 0.0498 Å. Dihedral angles between the center and terminal pyridine rings of the terpyridine ligands are only 3.39° and 2.87°. The mean angle between the two terpyridines is 95.4°, thus almost orthogonal. Figure 2 shows the molecular packing along the *c* axis and the arrangement of the Ru atoms in the crystal structure of unreduced compound **1**. The shortest distance between Ru centers is 8.943 Å along the *b* axis. Unreduced compound **1** has two PF_6^- ions and one $[(CH_3)_2CO]$ present per molecule. The closest distance between a Ru atom and a PF_6^- ion is 5.692 Å, while the acetone molecule is located about 6.7 Å from the Ru atom. The PF_6^- anions and the acetone preclude short intermolecular contacts between the $[Ru(terpy)_2]^{2+}$ molecules along the *c* axis.

Table 2. Selected Bond Lengths (Å) and Angles (deg)

		1	
compd	$1\cdot(PF_6)_2[(CH_3)_2CO]$	site A	site B
	Bond Lengths (Å)		
Ru−N(1)	2.07(1)[a]	2.06(1)	2.07(1)
Ru−N(4)	1.99(1)	1.98(1)	1.99(1)
Ru−N(7)	2.05(1)	2.05(1)	2.08(1)
N(1)−C(2)	1.37(2)	1.42(2)	1.38(2)
N(4)−C(3)	1.34(2)	1.35(2)	1.38(2)
C(2)−C(3)	1.47(2)	1.42(2)	1.40(2)
N(4)−C(5)	1.38(1)	1.33(2)	1.34(2)
N(7)−C(6)	1.37(2)	1.40(2)	1.40(2)
C(5)−C(6)	1.43(2)	1.42(2)	1.45(2)
Ru−N(19)	2.09(1)	2.08(1)	2.061(9)
Ru−N(22)	1.96(1)	2.00(1)	1.99(1)
Ru−N(25)	2.07(1)	2.09(1)	2.06(1)
N(19)−C(20)	1.36(2)	1.39(2)	1.37(2)
N(22)−C(21)	1.38(2)	1.38(2)	1.35(2)
C(20)−C(21)	1.46(2)	1.44(2)	1.41(2)
N(22)−C(23)	1.31(1)	1.35(2)	1.37(2)
N(25)−C(24)	1.39(2)	1.36(2)	1.38(2)
C(23)−C(24)	1.48(2)	1.40(2)	1.41(2)
	Bond Angles (deg)		
N(1)−Ru−N(4)	78.3(4)	79.4(4)	79.2(4)
N(4)−Ru−N(7)	79.3(4)	78.7(4)	79.0(4)
N(1)−Ru−N(19)	90.0(4)	88.6(4)	86.9(4)
N(1)−Ru−N(22)	101.4(4)	96.9(4)	105.8(4)
N(1)−Ru−N(25)	93.8(4)	97.7(4)	96.4(4)
N(4)−Ru−N(19)	102.7(4)	101.1(4)	102.0(4)
N(4)−Ru−N(22)	177.5(4)	176.4(4)	174.9(5)
N(4)−Ru−N(25)	98.6(4)	101.6(4)	100.0(4)
N(7)−Ru−N(19)	94.2(4)	96.7(4)	97.4(4)
N(7)−Ru−N(22)	101.0(4)	104.9(4)	95.9(4)
N(7)−Ru−N(25)	90.4(4)	85.6(4)	87.6(4)

[a] Numbers in parentheses are estimated standard deviations in the least significant digits.

As part of the analysis of our X-ray crystal structure, we searched for intermolecular contacts.[17,18] The distance between two molecules was calculated by d (Å) = distance$(X_1-X_2) \times \cos\theta$, where X_1 and X_2 correspond to the molecular centers of each π orbital, and θ is the angle between two molecular centers. The structure of unreduced **1** exhibits several close intermolecular interactions. Most intermolecular contacts occur between terpyridine ligands along the *b* axis where the shortest distance between the Ru centers is 8.943 Å. The two closest distances for the intermolecular contacts are 4.143 and 4.257 Å. Another intermolecular contact occurs between two ligands along the *c* axis with a distance of 4.9 Å. A third intermolecular contact is observed also along the *c* axis, but the distance of between X_1 and X_2 is too big (5.207 Å) to account for a true intermolecular contact.

Crystal Structure of 1. Compound **1** was obtained by reductive electrocrystallization of $1\cdot(PF_6)_2$. Noticeably, the

(16) (a) Wagner, M. J.; Dye, J. L. *J. Solid State Chem.* **1995**, *117*, 309. (b) Dye, J. L.; Wagner, M. J.; Overney, G.; Huang, R.; Nagy, T. F.; Tomanek, D. *J. Am. Chem. Soc.* **1996**, *118*, 7329. (c) Huang, R. H.; Wagner, M. J.; Gilbert, D. J.; Reidy-Cedergren, K. A.; Ward, D. L.; Faber, M. K.; Dye, J. D. *J. Am. Chem. Soc.* **1997**, *119*, 3765.

(17) (a) Paliwal, S.; Geib, S.; Wilcox, C. S. *J. Am. Chem. Soc.* **1994**, *116*, 4497. (b) Miyamura, K.; Mihara, A.; Fujii, T.; Gohshi, Y.; Ishii, Y. *J. Am. Chem. Soc.* **1995**, *117*, 2377. (c) Weiss, H.-C.; Bläser, D.; Boese, R.; Doughan, B. M.; Haley, M. M. *Chem. Commun.* **1997**, 1703. (d) Yoshida, N.; Shio, H.; Ito, T. *Chem. Commun.* **1998**, 63.

(18) (a) Hanton, L. R.; Hunter, C. A.; Purvis, D. H. *J. Chem. Soc., Chem. Commun.* **1992**, 1134. (b) Hunter, C. A.; Sanders, J. K. M. *J. Am. Chem. Soc.* **1990**, *112*, 5525. (c) Hunter, C. A.; Singh, J.; Thornton, J. M. *J. Mol. Biol.* **1991**, *218*, 837.

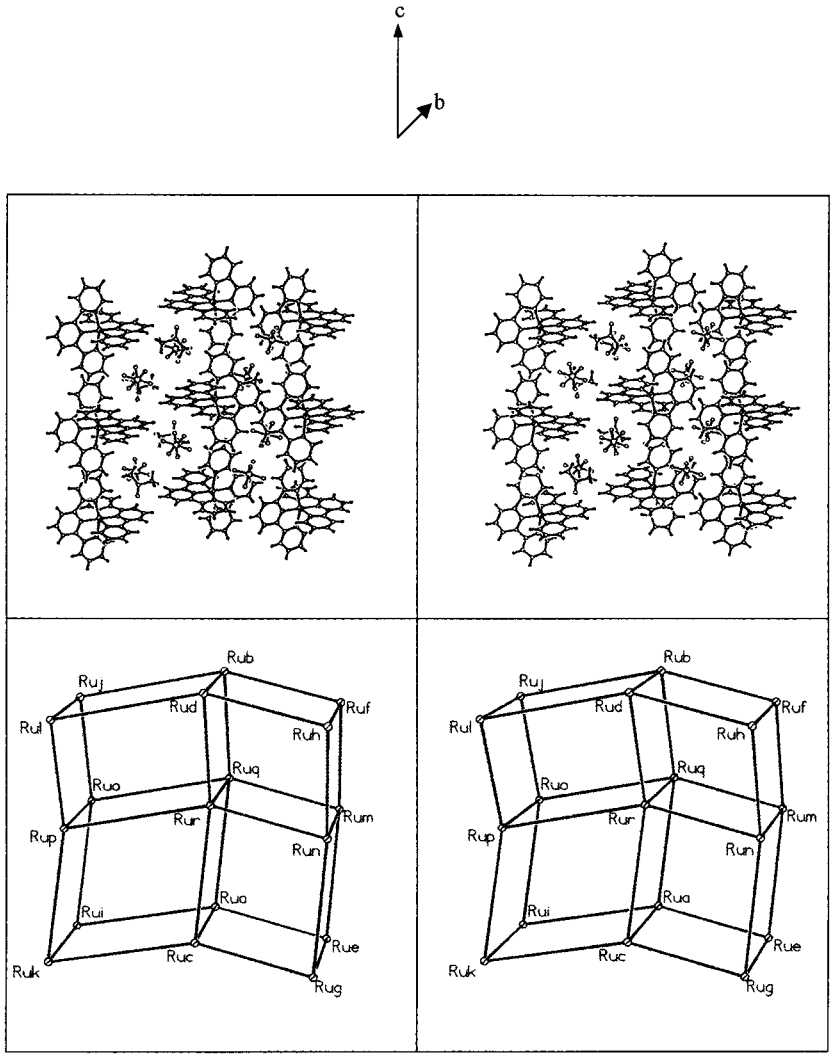

Figure 2. Molecular packing along the *c* axis of the lattice for unreduced compound **1**. The bottom of the figure shows only the positions of the Ru centers.

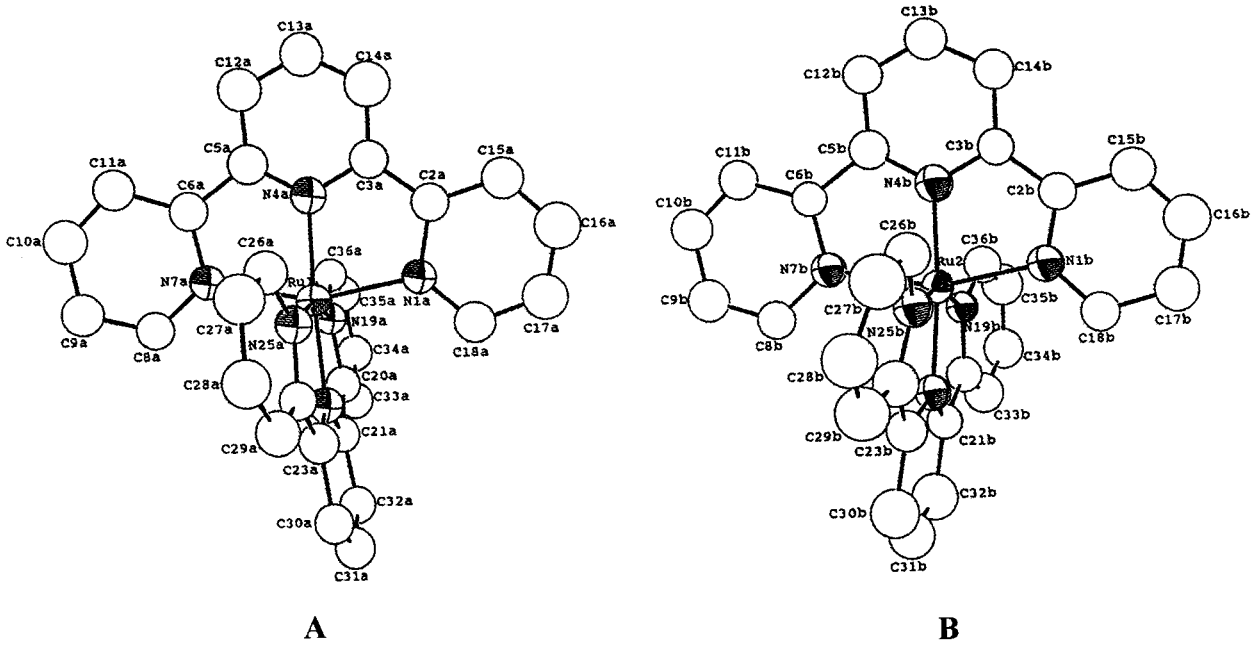

Figure 3. ORTEP view of the two crystallographic $[Ru(terpy)_2]^0$ units (A and B) in the unit cell of crystal **1**. The hydrogens have been omitted for clarity. Thermal ellipsoids are drawn at 50% probability.

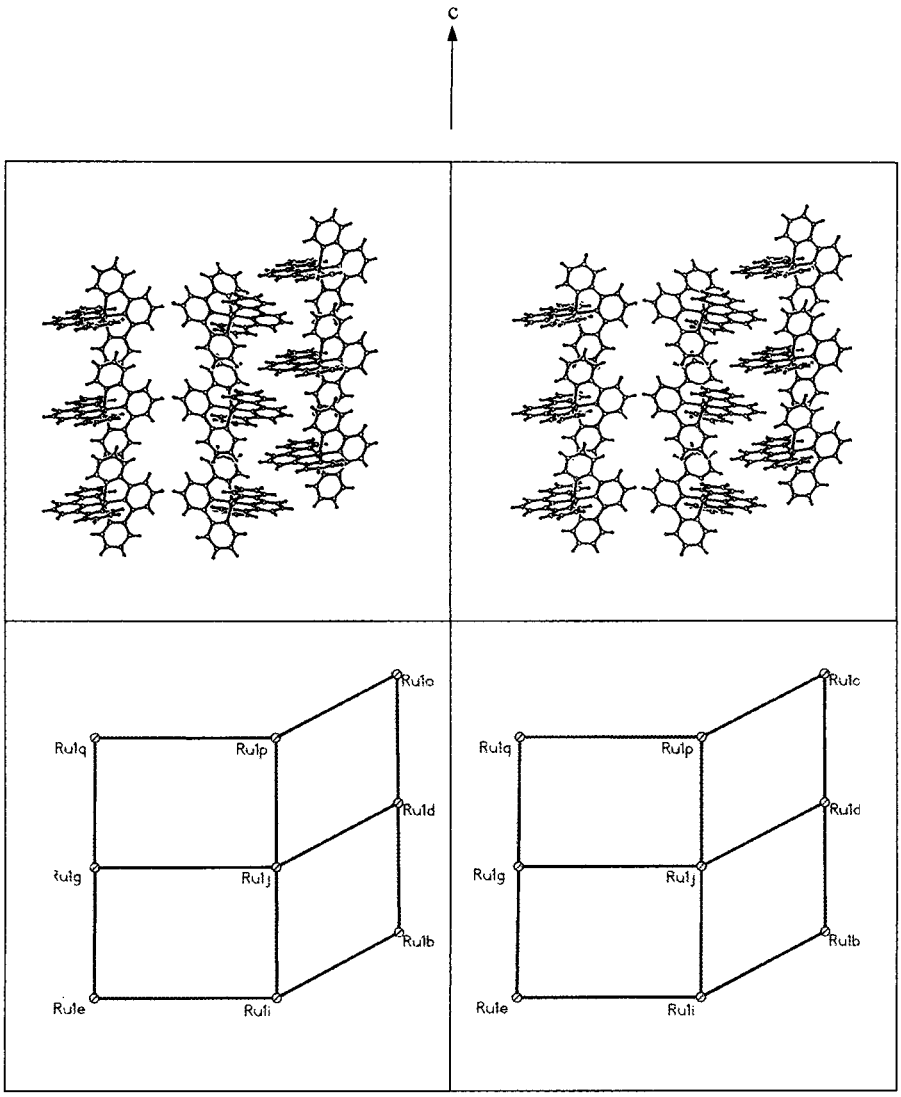

Figure 4. Molecular packing along the *c* axis for compound **1**. The bottom of the figure shows only the positions of the Ru centers.

crystals show no counteranions (PF_6^-) or [$(CH_3)_2CO$] in the lattice, a significant difference from unreduced **1**. Consequently, the material is exclusively composed of $[Ru(terpy)_2]^0$. The crystal system is orthorhombic with space group *Fdd*2. The unit cell was determined to be a black rod-shaped crystal (0.15 × 0.18 × 0.42 mm). Figure 3 presents the two crystallographically independent $[Ru(terpy)_2]^0$ units, A and B. The N4a−Ru1−N22a angle for unit A is 176.4°, and it is 185.1° for unit B, this being the only substantial difference between A and B. Other differences between A and B are negligible. Selected bond lengths and angles are summarized in Table 2. All terpyridine ligands are substantially the same and almost perfectly planar for reduced compound **1**. The mean deviations from the planes of each terpyridine ligand are 0.0702 and 0.0435 Å for A and 0.0352 and 0.0404 Å for B. Dihedral angles between the center pyridine ring and the terminal pyridine rings of the terpyridine ligands are 4.39° and 1.79° for A and 4.83° and 0.68° for B. From a comparison of the molecular structures of unreduced **1** and reduced **1**, the latter shows a higher degree of distortion from octahedral symmetry. Another small but significant difference between the structures of $[Ru(terpy)_2]^{2+}$ and $[Ru(terpy)_2]^0$ exists in the C(2)−C(3) and N(4)−C(5) distances. The bond lengths observed for reduced **1** are shorter by 0.05 and 0.04 Å for each C(2)−C(3) and N(4)−C(5) than for unreduced **1**. This bond shortening upon reduction was also observed for $[Ru(bpy)_3]^0$.[4] The shortening of the C(2)−C(3) bond could indicate some degree of electron localization on the terpyridine ligands.

Figure 4 shows a view along the *c* axis of the molecular packing and the arrangement of the Ru atoms in the crystal structure of **1**. $[Ru(terpy)_2]^0$ units show clear intermolecular contacts down the *c* axis. The closest Ru−Ru distance between these stacks is 8.507 Å, which is shorter than for unreduced **1** (8.943 Å). There are three specific intermolecular interactions that have been identified with about a 3.5 Å distance. As depicted in Figure 4, all of the interactions occur between intermolecular stacks along the *c* axis. One of them occurs between the interdigitated stacks, see Figure 4. The average distance between these interstacked terpy ligands is 3.67 Å. Another close contact occurs between intermolecular terminal pyridines within a single running parallel stack, down the *c* axis. The middle stack composed of three $[Ru(terpy)_2]^0$ units in Figure 4 is shown expanded in Figure 5. These three units are essentially arranged in a pattern similar to that observed and reported by Lehn's group for some rack-type Ru complexes.[19] The terminal pyridine ring of C6−N7−C8−C9−C10−C11

(19) (a) Hanan, G. S.; Arana, C. R.; Lehn, J.-M.; Fenske, D. *Angew. Chem., Int. Ed. Engl.* **1995**, *34*, 1122. (b) Hanan, G. S.; Arana, C. R.; Lehn, J.-M.; Baum, G.; Fenske, D. *Chem.—Eur. J.* **1996**, *2*, 1292.

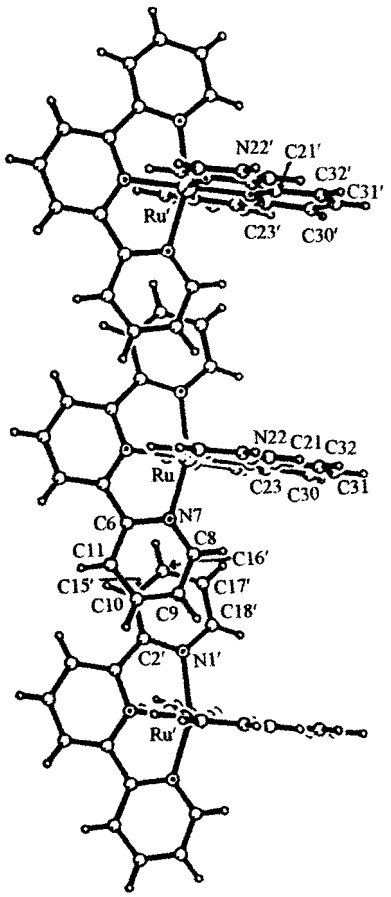

Figure 5. View of a single molecular stack of $[Ru(terpy)_2]^0$ along the *c* axis.

stacks with the other terminal pyridine of an adjacent molecule (N1′−C2′−C15′−C16′−C17′−C18′), thus forming an infinite array along the *c* axis. The distance between these terpy ligands is 3.45 Å. We also investigated centroid-to-centroid distances between intermolecular terpyridine ligands that lie perpendicular to the *c* axis. From Figure 5, the centroid-to-centroid distance between the center pyridines (the ring of C21−N22−C23−C30−C31−C32 and the ring of C21′−N22′−C23′−C30′−C31′−C32′) is 8.507 Å. The intermolecular terpyridine ligands along the *c* axis are perfectly parallel to each other.

When comparing structures and molecular packings of **1** and its parent complex, unreduced **1**, an important consideration is the location and the possible distorting effect of the additional electron density in the former. $[Ru(terpy)_2]^0$ has two additional electrons substituting the two PF_6^- anions. In contrast with cryptatium[6] and the one electron reduced binaphthyridine-ruthenium complex, $[Ru(binap\text{-}2)_3](PF_6)$ (Chart 2),[3] which exhibit large distortions due to the added electron, no significant distortion of the intrinsic geometry around the central Ru atom is observed for **1**. In our previous paper,[4] a similar observation was made for $[Ru(bpy)_3]^0$, despite the fact that the predicted distortion was larger because the number of reduction electrons (2) did not match the number of bipyridine ligands (3). In the present case the number of reduction electrons (2) is equal to the number of ligands (2), so a more symmetrical reduced structure was anticipated. One possible explanation for the observations with $[Ru(bpy)_3]^0$ is that the additional electrons are localized in an orbital that has equal contributions from all ligands. Another possible interpretation is that the reduction electron density, or a part of it, remains in some lattice sites. In this case the crystalline material could be described as an "electride", at least partially. Interestingly, analysis of the crystal packing of $[Ru(terpy)_2]^0$ reveals the presence of "empty" cavities which could harbor electron density as in the case of electrides. These intermolecular spaces, which are empty cavities in the lattice structure, can be easily seen in Figure 6a. They correspond to the approximate positions where the PF_6^- ions are located in the structure of unreduced **1**.

To investigate the empty cavities in the lattice structure, it is necessary to visualize the void spaces in the crystal structures and to determine the diameters, lengths, and geometries of the channels. We used a combination of the Fortran program VOID and a commercial isosurface 3D-display program, EXPLORER, to represent the empty spaces in the crystalline structure and to visualize the channels and cavities from a variety of views. The calculation using the program "xeo" displays the empty cavities and channels, while the calculation by the program "zeo"

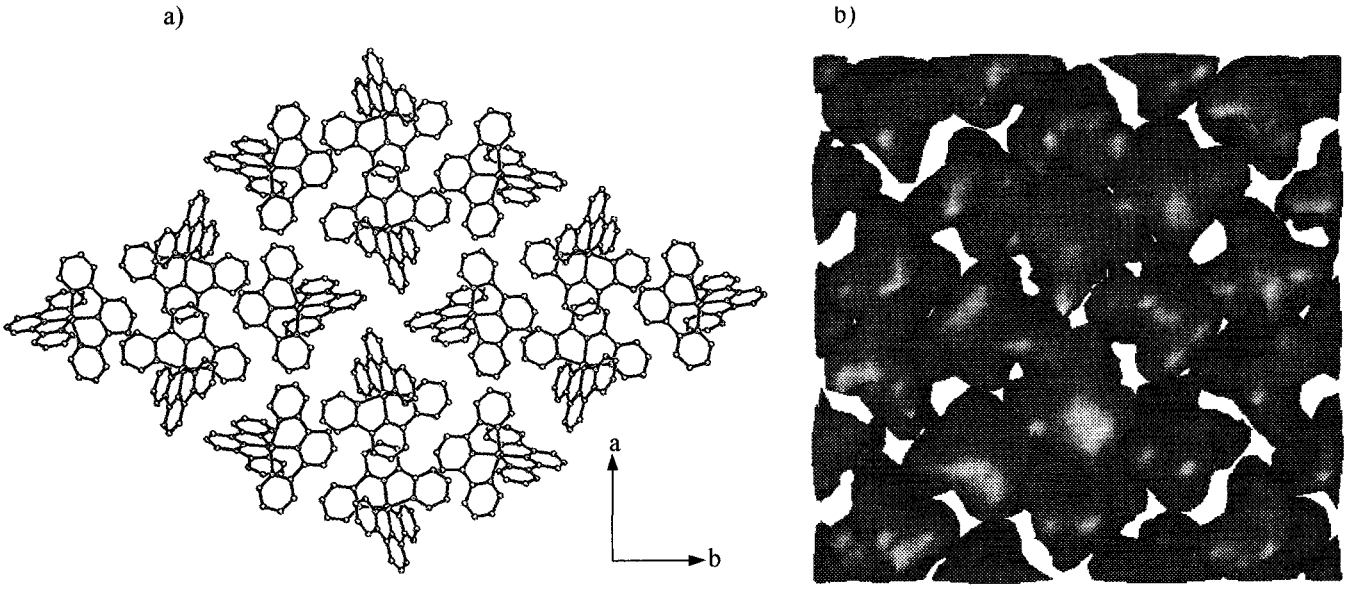

Figure 6. (a) Projection of the lattice structure of **1** looking down the *c* axis: the hydrogen atoms are omitted for clarity. Empty intermolecular spaces exist around the middle of the projection shown. (b) View down the *c* axis calculated from the positive molecular packings of $[Ru(terpy)_2]^0$ crystals. Empty spaces are white.

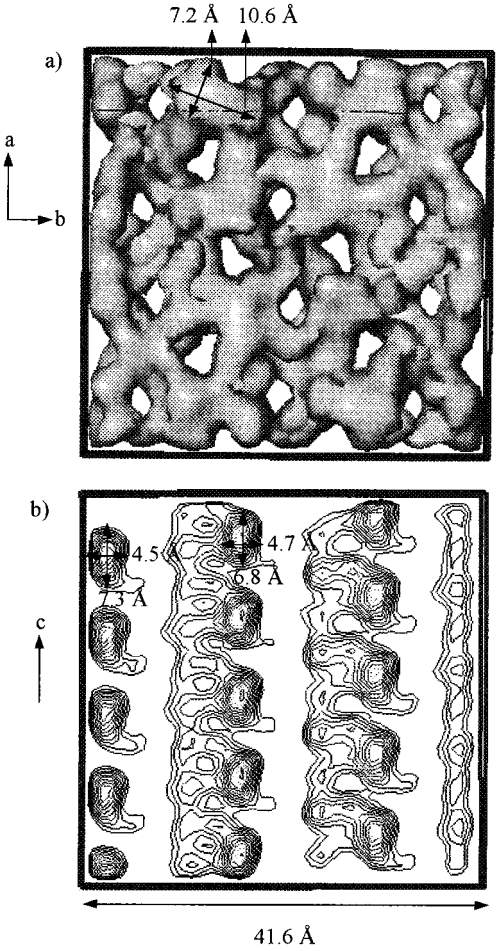

Figure 7. $[Ru(terpy)_2]^0$ crystals. (a) View down the *c* axis calculated from the negative molecular packings. Black portions represent empty spaces. (b) View along the *c* axis. The contour lines define the cavities.

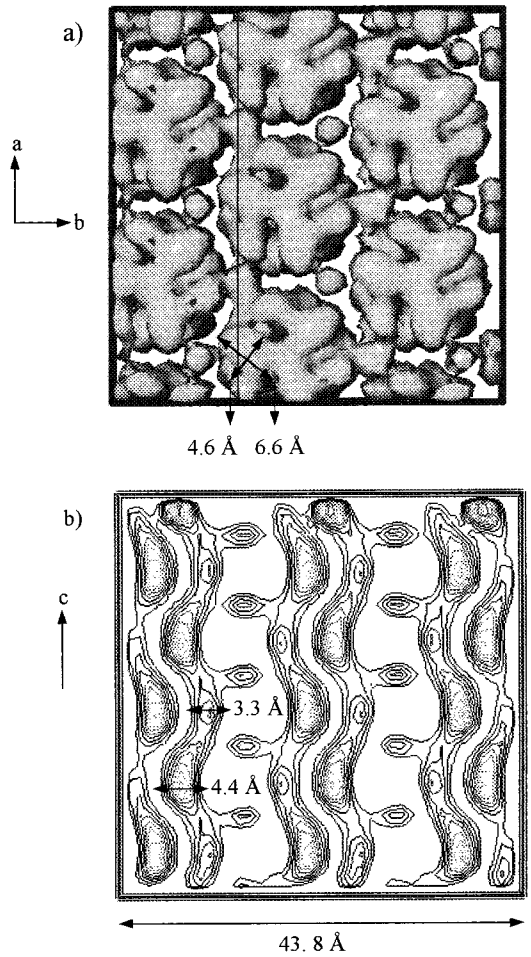

Figure 8. $[Ru(bpy)_3]^0$ crystals. (a) View down the *c* axis calculated from the negative molecular packings. Black portions represent empty spaces. (b) View along the *c* axis. The contour lines define the cavities.

displays the atomic or molecular surfaces. In principle, a small distance parameter of the isosurface, called molecular van der Waals surface, would give the true channel and cavity shapes. Figure 6b shows the molecular packing of $[Ru(terpy)_2]^0$ (**1**) along the *c* axis, using a 0.42 Å distance from the molecular van der Waals surfaces. When we look down the *c* axis, the cavity holes (white parts in Figure 6b) are clearly delineated. The cavity sizes are 6.8 × 4.7 and 4.5 × 7.3 Å. The channels are calculated from the negative molecular packings. Figure 7a shows the cavities of $[Ru(terpy)_2]^0$ down the *c* axis. One of the oval-shaped cavities is 7.2 × 10.6 Å, measured on the *a,b* plane. Figure 7b shows a cut of these surfaces along the *c* axis. We have also analyzed the packing structure of $[Ru(bpy)_3]^0$ and compared it to that of $[Ru(terpy)_2]^0$. Figure 8a shows the empty cavities found in $[Ru(bpy)_3]^0$ down the *c* axis. The size of the oval-shaped cavity is 6.6 × 4.6 Å. Figure 8b displays a cut of the surface down the *c* axis, clearly showing that channels are also present along the *c* axis, with diameters of 3.3 and 4.4 Å. The Dye group recently reported that the simplest electride, cesium metal (IV), has 2.3 Å diameter cavities and large channels with 1.7 and 1.9 Å diameters that connect the cavities to form a 3D array.[15b] In comparison to this electride, the reduced compounds $[Ru(terpy)_2]^0$ and $[Ru(bpy)_3]^0$ have relatively large cavities and channels. These materials can thus probably be classified as electrides, only on the basis of the size of the intermolecular spaces in the lattice structure. However, it is not possible to judge where the extra electron density is localized solely on the basis of the crystal structure. Spectroscopic and transport studies of these materials are currently being measured in an effort to evaluate their properties and to gain additional insight about the nature of the added electron density.

Acknowledgment. The authors wish to thank the National Science Foundation (Grants DMR-9803088 and CHE-9313018) for providing financial support for this work.

Supporting Information Available: Tables of crystal data and structure refinement, anisotropic thermal parameters, bond lengths and angles, and hydrogen atom coordinates for **1** and **1**·$(PF_6)_2[(CH_3)_2$-CO]. This material is available free of charge via the Internet at http://pubs.acs.org.

IC981395E